

Phase shifts, image planes, and surface states at metal surfaces

M. Ortuño

Departamento de Física, Universidad de Murcia, E-30001 Murcia, Spain

P. M. Echenique*

Cavendish Laboratory, University of Cambridge, Cambridge CB3 0HE, England, United Kingdom

(Received 18 April 1986)

Crystal- and image-potential-induced surface states of Cu, Ag, and Ni are studied with use of the phase-analysis model, with an accurate expression for the classical image-barrier phase shift. The energies of the first three surface states of the (111) and (001) faces of these metals are obtained as a function of the image plane distance to the surface, z_{im} . The experimental results are reproduced if a small effective z_{im} is used. The effects of changing the plateau of the image potential are also analyzed.

I. INTRODUCTION

The experimental detection of image-potential-induced surface states has aroused new interest in the factors determining the binding energies of surface states in general.¹⁻⁶ Multiple-reflection theory has been particularly successful in explaining in a simple and accurate way the "crystal-induced" surface states and the Rydberg series produced by the long-range image potential. In this theory, also referred to as phase-analysis model, both types of surface states naturally appear on the same footing.⁷⁻⁹

The aim of this paper is to present a new multiple-reflection calculation of surface states using an accurate expression for the phase change produced by the image-potential barrier. We also analyze the effects of changing the image plane distance to the surface and the depth of the plateau in the image potential. We use nearly-free-electron theory to obtain the phase shift produced by the crystal barrier and an approximation due to Wannier to calculate the image-barrier phase shift. The model is applied to study the surface states of copper, silver, and nickel.

Some authors have paid attention to the effects associated to the variation of the crystal potential in the direction parallel to the surface.¹⁰ These effects can be incorporated in a natural way in the multiple-reflection scheme of Echenique and Pendry⁷ by introducing a parallel dependence of the crystal phase shift ϕ_c . Thus, the so-called "phase analysis" and "surface corrugation" models do not constitute alternative models. Besides, Pendry *et al.*¹¹ have shown that corrugation effects in silver do not lead to appreciable effects neither on the binding energies nor on the effective mass parallel to the surface for the image states. Similar conclusions have been reached by Hulbert *et al.* for the unoccupied image states on Cu.¹²

The outline of the paper is as follows. In Sec. II, we describe, in some detail, the model that we are going to use obtaining the phase shifts produced by the crystal- and by the image-potential barrier. In Sec. III, we apply

the model to calculate the binding energies of the first three surface states of the (111) and the (001) faces of copper, silver, and nickel. This calculation is done as a function of the image plane distance to the surface and for two values of the saturation plateau of the image potential. Finally, in Sec. IV, we discuss the results and extract some conclusions.

II. DESCRIPTION OF THE MODEL

The first question to decide in the construction of the model is which one-electron potential to use in the effective Schrödinger equation for the surface states. This is, of course, a simplification of the many-body problem occurring in reality. The surface screening and other many-body effects are simulated by a suitable one-electron potential. Several model potentials exist in the literature.¹³ While self-energy based calculations are asymptotically correct, but not very reliable close to the surface, the density functional formalism is not adequate in the asymptotic limit, but provides very precise results at short distances. We will assume that the potential inside the crystal is the same as for the bulk and abruptly terminates at half an interlayer from the last layer of surface atoms. Outside the crystal we consider a flat potential merging into an imagelike Coulomb potential, which we know has the correct asymptotic behavior. In Fig. 1 we schematically show the model potential that we are going to use. The two arbitrary parameters of this model potential are the depth of the flat region and its width, or, equivalently, the distance of the image plane to the surface, z_{im} . Echenique and Pendry⁷ chose a potential outside the surface that matches into the crystal inner potential. However, in some references,² the flat potential is matched into the inner potential modulated by the \mathbf{g} Fourier component of the crystal potential $V_{\mathbf{g}}$, where \mathbf{g} is the reciprocal lattice vector opening the gap whose surface states we want to study. Because of that, we will consider two extreme depths for the plateau, i.e., equal to the bulk inner potential and equal to this plus the Fourier component $V_{\mathbf{g}}$. These two plateau levels are represented in Fig. 1.

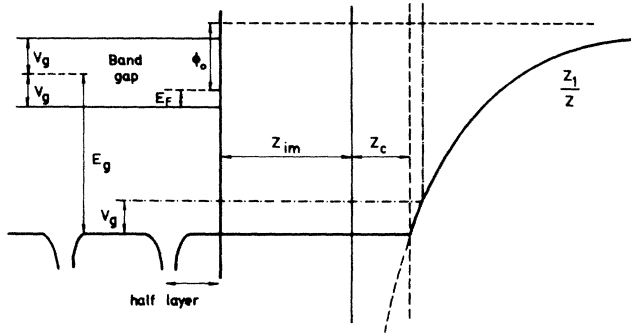


FIG. 1. Schematic representation of the potential in the vicinity of the surface. The parameters of the model V_g , E_g , E_F , ϕ_0 , z_{im} , and z_c are represented. The two plateau levels of the image potential are also drawn.

In the phase-analysis model one treats the states as electron waves undergoing multiple reflection between the crystal and the image potentials. Following Echenique and Pendry's nomenclature,⁷ we denote by ϕ_c and ϕ_b the phase changes between incident and reflected waves, produced by the crystal and the image potentials, respectively. Bound states occur when the sum of ϕ_b and ϕ_c is a multiple of 2π , which is a Bohr-like quantization condition on the round-trip phase accumulation.

The phase change produced by any general potential barrier is given by

$$\phi = 2 \tan^{-1} \left[\frac{\psi'(z_0)}{k\psi(z_0)} \right], \quad (1)$$

where z_0 is the value of the coordinate perpendicular to the surface z at the boundary of the barrier, $\psi(z)$ is the convergent solution of Schrödinger equation inside the barrier, $\psi'(z)$ is its derivative with respect to z , and k is the wave vector right outside the barrier. Equation (1) is obtained by matching both the wave functions and their derivatives outside and inside the barrier.

Let us consider first the phase change due to the image-potential barrier. The Schrödinger equation for this potential corresponds to the radial equation for the s states of the hydrogenic problem. Therefore, the solution convergent at infinity is the Whittaker function

$$W_{\lambda, 1/2}(2Z_1 z/\lambda),$$

where λ is defined as $Z_1/\sqrt{2|E|}$, and Z_1 is the multiplying coefficient in the $1/z$ potential, which is equal to $\frac{1}{4}$ for metals. For numerical purposes, we will use Wannier's approximation to $W_{\lambda, 1/2}$ (Ref. 14),

$$F_\lambda(y) = y [J_1(y) \cos(\lambda\pi) + N_1(y) \sin(\lambda\pi)], \quad (2)$$

where $y = (8Z_1 z)^{1/2}$. From Eqs. (1) and (2) we obtain for the image-barrier phase change,

$$\phi_b = 2 \tan^{-1} \left[\frac{4Z_1 J_0(y) \cos(\lambda\pi) + N_0(y) \sin(\lambda\pi)}{ky J_1(y) \cos(\lambda\pi) + N_1(y) \sin(\lambda\pi)} \right]. \quad (3)$$

In Fig. 2 we represent ϕ_b , as given by Eq. (3), as a func-

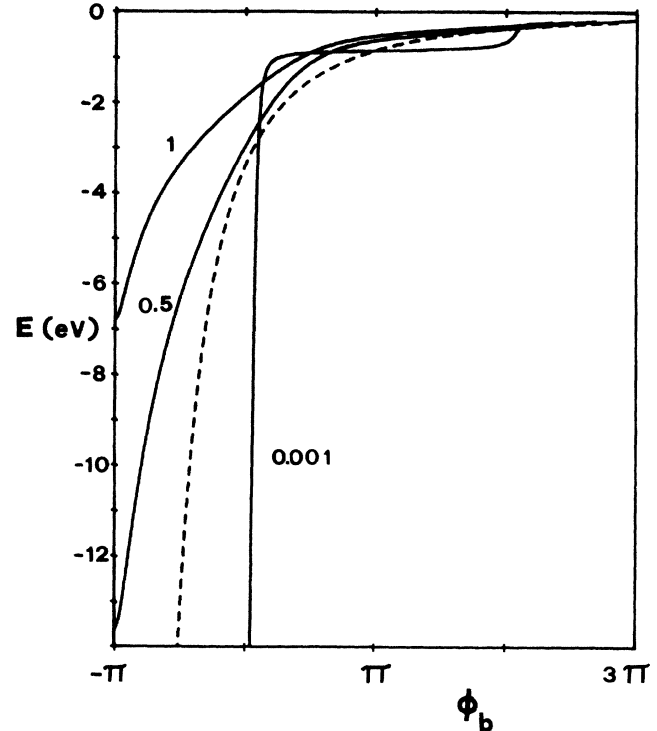


FIG. 2. Energy variation of the image-potential phase shift ϕ_b as given by Eq. (3), for three values of z_c , $z_c = 0.001, 0.5$, and 1 . The dashed lines correspond to ϕ_b as given by Eq. (5).

tion of energy for different cutoff distances z_c (see Fig. 1). In the hydrogenic limit, i.e., when $z_c \rightarrow 0$, ϕ_b tends towards a set of steps at the energies

$$E_n = -\frac{Z_1^2}{2n^2} \quad (n = 1, 2, \dots). \quad (4)$$

Of course, in the asymptotic limit, ϕ_b from Eq. (3) reproduces the hydrogenic series. Increasing z_c , the curves for ϕ_b become smoother. In Fig. 2, also represented (dashed line) is the curve

$$\phi_b = \left[\frac{1}{\sqrt{8|E|}} - 1 \right] \pi \quad (5)$$

often used in the literature^{3,6,8,9} as an approximation to the image-barrier phase change. It corresponds to the Wentzel-Kramers-Brillouin (WKB) approximation for ϕ_b and it clearly defers from the more accurate expression, Eq. (3). As we will see, all the surfaces studied correspond to z_c close to 0.5 a.u. For this value of z_c , ϕ_b is already quite flat, so we do not expect very large differences between using Eqs. (3) or (5) for ϕ_b . However, these differences become appreciable for the corresponding derivative functions, as it has been clearly pointed out by McRae and Kane.¹⁵ This is important because these functions are related to the lifetime of the state as shown by Echenique¹⁶ and by Echenique and Pendry.^{7,13} The curve for ϕ_b in Fig. 2 corresponding to $z_c = 0.5$ a.u. is rel-

atively similar to what Smith calls "experimental" curve for ϕ_b . Both the steplike and the imagelike behavior of this curve are naturally included in our ϕ_b . We have also calculated ϕ_b using a more elaborated approximation for $W_{\lambda,1/2}$, also given by Wannier,¹⁴ obtaining no significant differences with respect to the value obtained from Eq. (3).

To calculate ϕ_c we consider the gap to be nearly-free-electron-like and the surface states within it to be of the form described by Goodwin.¹⁷ For the sake of simplicity, we only analyze gaps opened by potential Fourier components corresponding to lattice vectors \mathbf{g} normal to the surfaces that we study. Following Smith,⁹ we find for ϕ_c ,

$$k \tan \left[\frac{\phi_c}{2} \right] = \frac{g}{2} \tan \left[\frac{\pi}{2} + \delta \right] - q, \quad (6)$$

where

$$\sin(2\delta) = -\frac{gq}{2V_g}, \quad (7)$$

$$\frac{1}{2}q^2 = (4EE_g + V_g^2)^{1/2} - (E + E_g), \quad (8)$$

E is the energy relative to the crystal inner potential and E_g is equal to $g^2/8$. We have used atomic units throughout ($\hbar = m = 1$). The origin of coordinates has been chosen on a surface atom and we are mainly interested in Shockley-inverted gaps, so that $V_g > 0$. The phase accumulated in the plateau,

$$2k(z_{im} + z_c),$$

has to be added to either ϕ_c or ϕ_b . This discussion completes the description of the method.

III. RESULTS

We have applied the model to study the surface states of Cu, Ag, and Ni associated with the bulk L gap for the (111) faces and with the bulk X gap for the (001) faces. Both the L and the X gaps are opened by potential components corresponding to reciprocal lattice vectors normal to the (111) and the (001) surfaces, respectively. The four needed parameters for the calculation are V_g , E_g , the Fermi energy E_F , and the work function ϕ_0 . They are all represented in Fig. 1. The first three parameters are obtained from the bulk band structures. V_g is taken as half the width of the gap that we are considering. E_g is the energy difference between the center of this gap and the crystal inner potential. The Fermi energy is measured with respect to the bottom of the gap. The work function is the difference between the vacuum level and the Fermi energy. The values of the parameters that we have used for the different surfaces are listed in Table I.^{3,9}

In Figs. 3, 4, and 5 we represent

$$\lambda = Z_1 / \sqrt{2|E|}$$

as a function of the image plane distance to the surface, z_{im} , for copper, silver, and nickel, respectively. The hydrogenic series corresponds to integer values of λ . The first three surface states of the (111) and the (001) faces are studied for each of the three metals considered. The solid lines, in the three figures, correspond to considering

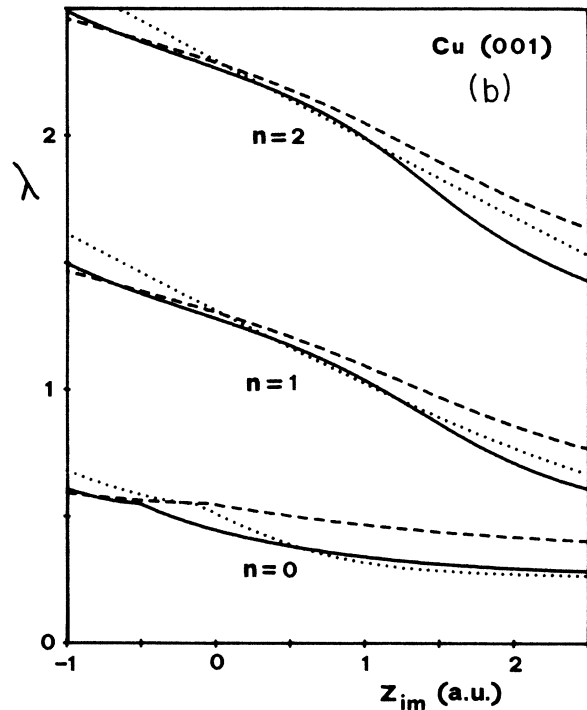
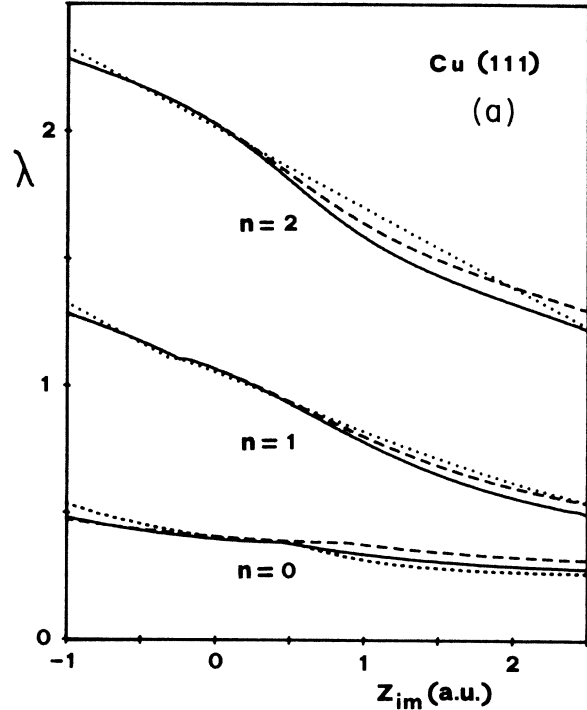


FIG. 3. Energy parameter λ as a function of z for Cu(111) and Cu(001). The solid lines correspond to the lower plateau of the potential and to using Eq. (3) for ϕ_b . The dashed lines are for the higher plateau and the dotted lines use Eq. (5) for ϕ_b .

the barrier plateau at the same energy as the bottom of the crystal potential, and using Eq. (3) for ϕ_b . The dashed lines are obtained by a similar calculation but considering the plateau at an energy V_g higher than before. They coincide with the results of Weinert *et al.*²

The dotted lines are obtained using the approximate expression for ϕ_b given by Eq. (5) and considering the same potential as for the solid lines. To obtain the fairly good

agreement between the solid and the dotted lines observed in Figs. 3–5, one has to consider that Eq. (5) includes the phase delay accumulated in the part of the plateau between the image plane and the Coulomb potential, i.e., $2kz_c$.

We can also note that the changes in the plateau level do not substantially alter the results for small z_{im} . The only exception is the $n=0$ surface state of Cu(001).

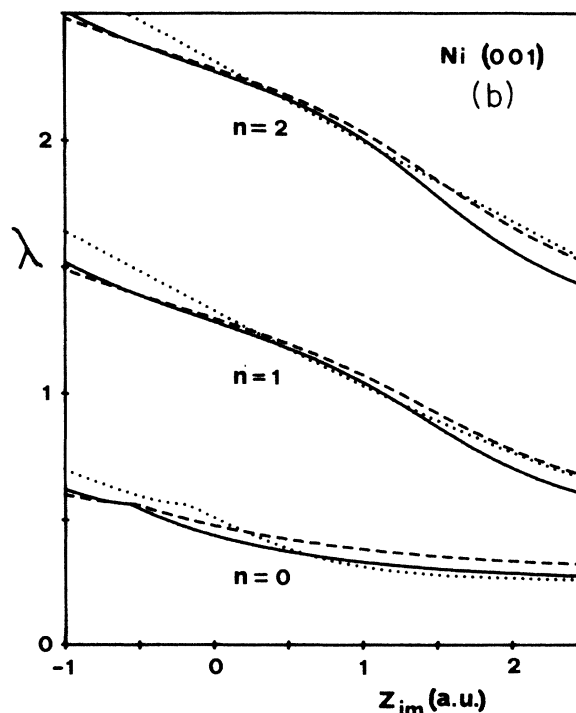
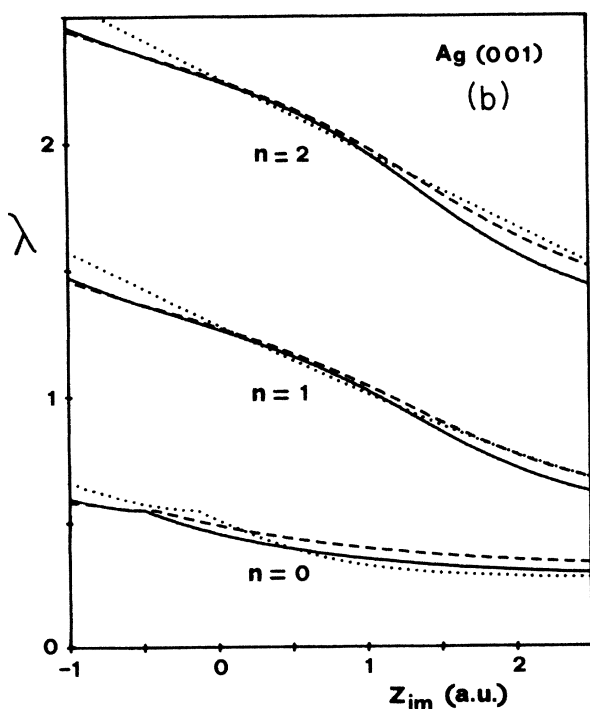
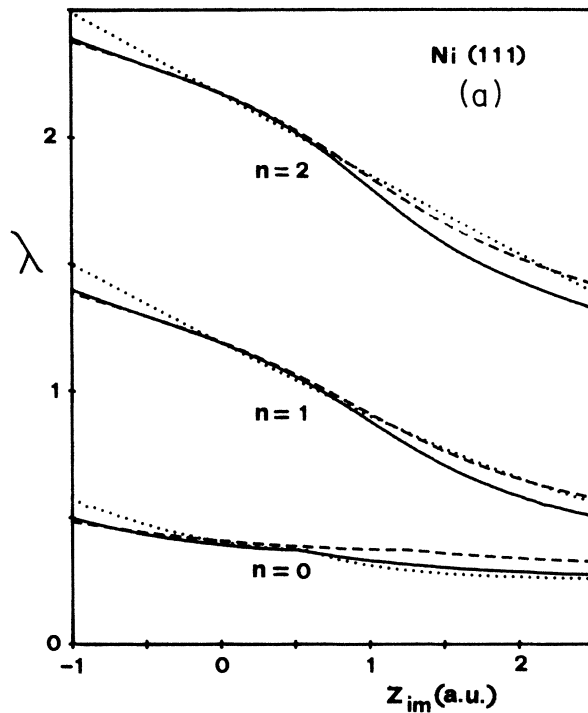
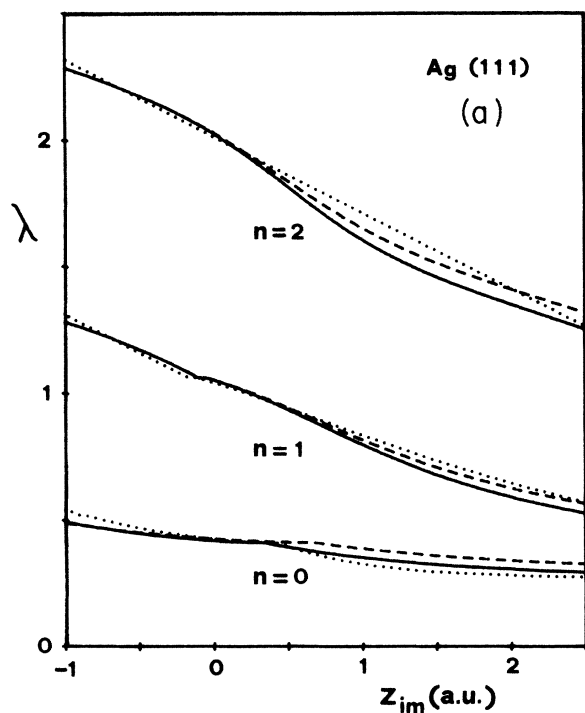


FIG. 4. Same as Fig. 3, but for Ag(111) and Ag(001).

FIG. 5. Same as Fig. 3, but for Ni(111) and Ni(001).

TABLE I. Summary of data for the (111) and (001) faces of Cu, Ag, and Ni. All energies are in eV. V_g , E_g , E_F , and ϕ_0 are the parameters used in our model. E (expt.) and E (theor.) are the experimental and theoretical values, respectively, of the surface state energies. z_{im} are the image plane distances that fit the experimental energies with our model.

Sample	V_g	E_g	E_F	ϕ_0	State	E		z_{im}	
						Expt.	Ref.		Theor.
Cu(111)	2.55	10.3	0.85	4.94	$n=0$	-0.39	18	-0.46	-0.45
					$n=1$	-0.94	6	-0.76	-0.5
Cu(001)	3.05	13.45	-1.8	4.59	$n=0$	1.15	19	0.2	-0.3
					$n=1$	-0.64	4	-0.52	-0.7
Ag(111)	2.15	9.64	0.31	4.74	$n=0$	-0.1	20	-0.16	-0.4
					$n=1$	-0.77	5	-0.78	-0.1
Ag(001)	2.53	12.1	-1.78	4.6	$n=0$			0.4	
					$n=1$	-0.5	21	-0.53	-0.2
Ni(111)	3.7	11.6	0.9	5.2	$n=0$	-0.2	22	-0.4	-0.1
					$n=1$	-0.6	23	-0.61	-0.05
Ni(001)	3.4	14.7	-2.53	5.2	$n=0$	0.7	24	0.7	0
					$n=1$	-0.4	23	-0.52	-0.7

In Table I we summarized the data for the (111) and (001) surfaces of copper, silver, and nickel. We start by listing the values of the parameters V_g , E_g , E_F , and ϕ_0 , used in our model.^{3,9} We then list the experimental results for the energies of the $n=0$ and 1 surface states. The energies corresponding to the $n=0$ states are measured with respect to the Fermi level, while all other energies are considered with respect to the vacuum level. The theoretical energies for the first three surface states, obtained using our model, are also given, considering $z_{im}=0$. These predictions are 1.5, 1.43, and 1.6 a.u. for Cu, Ag, and Ni, respectively. All energies above are given in electron volts. Table I ends up giving the values of z_{im} that will reproduce, within our model, the experimental energies of the $n=0$ and 1 surface states.

In Table II we compare the results of the phase-analysis model for two different expressions of ϕ_b , Eqs. (3) and (5). We do that for Ag(111) and Ni(001). The three (111) surfaces considered in this paper present similar results and the same occurs for the (001) surfaces. We compare the binding energies obtained with both methods, taking

$z_{im}=0$, and the derivatives of ϕ_b with respect to energy, taken at their corresponding binding energies. The differences for the binding energies are fairly small, especially for the (111) faces, but they are relatively important for $(\partial\phi_b/\partial E)|_{E_b}$ and therefore for the lifetimes.²⁵

IV. DISCUSSION AND CONCLUSIONS

We first notice that in our model potential the experimental values are reproduced for values of z_{im} smaller than the ones quoted by Lang and Kohn.²⁶ Although at first sight this might be surprising, it contains, however, the correct physics of the problem and is consistent with recent studies of many-body effects in the binding energies of image states at surfaces. Bausels and Echenique²⁷ have shown that if one defines a local effective one-body potential in the manner prescribed by Manson and Ritchie²⁸ in their self-energy formalism, the effects of plasmon dispersion (defining the image plane position) and high momentum single-particle excitations (leading to

TABLE II. Comparison of the phase-analysis model using two different expressions for ϕ_b , Eqs. (3) and (5). $E_v - E$ are the binding energies measured with respect to the vacuum level and $(\partial\phi_b/\partial E)$ are the derivatives with respect to the energy of ϕ_b .

Sample	State	$E_v - E$ (eV)		$\frac{\partial\phi_b}{\partial E}$ (eV ⁻¹)	
		Eq. (3)	Eq. (5)	Eq. (3)	Eq. (5)
Ag(111)	$n=0$	4.9	4.74	0.50	0.28
	$n=1$	0.78	0.79	3.7	4.12
	$n=2$	0.21	0.21	24.8	30.1
Ni(001)	$n=0$	4.5	3.4	0.6	0.46
	$n=1$	0.52	0.49	13.0	8.44
	$n=2$	0.17	0.16	70	45.3

a finite value of the effective potential at the origin) can be neglected when realistic values of the surface-plasmon dispersion relation are used. A simple but qualitatively correct description of this cancellation has been recently given by Giesen *et al.*²⁹ Note that this does not mean that the image plane positions are much smaller than the ones calculated by Lang and Kohn. The asymptotic expansion of the image potential can be derived from the Taylor expansion of the surface response function in powers of momentum parallel to the surface. The coefficient of the linear term, defining the image plane, can be chosen, as done by Bausels and Echenique,²⁷ to reproduce Lang and Kohn's values for the image plane position. What this means is that if an effective potential, evaluated from an undispersed response function, is used in regions outside the validity of the asymptotic value, no image plane shift should be included. This is the reason for which our theoretical values for the surface state energies are too high if we use for z_{im} the predictions by Lang and Kohn. This, of course, is still true for the potential used by Weinert *et al.*,² as can be seen in Figs. 3–5 (dashed lines).

We should like to emphasize that because of the above, our calculations with such simple models cannot be used to extract information about the image plane position. In fact, the whole model might be too simple, but its importance relies on the correct description of the systematics and trends of the binding energies and lifetimes of both crystal-induced and image-potential-induced surface states.

The model also gives information about the lifetimes of the surface states, which are related to the penetration of the wave functions in the material and so to the derivatives of ϕ_b with respect to energy taken at the resulting

binding energies.²⁵ ($\partial\phi_b/\partial E$) as a function of energy presents a series of peaks when we use Eq. (3) for ϕ_b . The positions of the binding energies in the gap determine the positions of the states in the peaks and so their lifetimes. The same is also true for the contribution of the bulk to the many-body corrections to the effective mass, due to the penetration of the wave function in the solid.

To conclude, we have studied theoretically the first three surface states of the (111) and (001) faces of Cu, Ag, and Ni. We have used the phase-analysis model, considering two different potentials and varying the image plane distance to the surface, z_{im} . We conclude that the results are fairly insensitive to changes in the plateau of the image potential. On the other hand, they strongly depend on z_{im} . To reproduce the experimental results one should use an effective z_{im} much smaller than the theoretical predictions by Lang and Kohn. We have used an accurate expression for the image-barrier phase shift ϕ_b and compared the results with those obtained with the ϕ_b normally used in the literature. The differences are not drastic, but they are big enough to recommend the use of the more accurate expression, which, at the same time, can be easily calculated. Then the model can correctly predict the trends in the binding energies and lifetimes of surface states.

ACKNOWLEDGMENTS

One of the authors (M.O.) would like to acknowledge the hospitality and financial support of the Theory of Condensed Matter (TCM) group of the Cavendish Laboratory, where part of the work was performed, while the other (P.M.E.) gratefully acknowledges help and support from Iberduero S.A. and the March Foundation.

*Present address: Euskal Herriko Unibertsitater Kimika, Donostia, Euskadi, Spain.

¹P. D. Johnson and N. V. Smith, *Phys. Rev. B* **27**, 2527 (1983).

²M. Weinert, S. L. Hulbert, and P. D. Johnson, *Phys. Rev. Lett.* **56**, 760 (1986).

³A. Goldmann, V. Dose, and G. Borstel, *Phys. Rev. B* **32**, 1971 (1985).

⁴D. Straub and F. J. Himpsel, *Phys. Rev. Lett.* **52**, 1922 (1984); D. Straub and F. J. Himpsel, *Phys. Rev. B* **33**, 2256 (1986).

⁵K. Giesen, F. Hage, F. J. Himpsel, H. J. Riess, and W. Steinmann, *Phys. Rev. Lett.* **55**, 300 (1985).

⁶S. L. Hulbert, P. D. Johnson, N. G. Stoffel, W. A. Royer, and N. V. Smith, *Phys. Rev. B* **31**, 6815 (1985).

⁷P. M. Echenique and J. B. Pendry, *J. Phys. C* **11**, 2065 (1978); see also P. M. Echenique, Ph.D. thesis, Cambridge University, 1976 (unpublished).

⁸E. G. McRae, *Rev. Mod. Phys.* **51**, 541 (1979).

⁹N. V. Smith, *Phys. Rev. B* **32**, 3549 (1985); N. V. Smith, *Appl. Surf. Sci.* **22**, 349 (1985); R. F. Garrett and N. V. Smith, *Phys. Rev. B* **33**, 3740 (1986).

¹⁰N. Garcia, B. Reihl, K. H. Frank, and A. R. Williams, *Phys. Rev. Lett.* **54**, 591 (1985).

¹¹J. B. Pendry, C. G. Larsson, and P. M. Echenique, *Surf. Sci.* **166**, 57 (1986).

¹²S. L. Hulbert, P. D. Johnson, M. Weinert, and R. F. Garrett, *Phys. Rev. B* **33**, 760 (1986).

¹³P. M. Echenique and J. B. Pendry, *J. Phys. C* (to be published).

¹⁴G. H. Wannier, *Phys. Rev.* **64**, 358 (1943).

¹⁵E. G. McRae and M. L. Kane, *Surf. Sci.* **108**, 435 (1981).

¹⁶P. M. Echenique, *J. Phys. C* **18**, L1133 (1985).

¹⁷E. T. Goodwin, *Proc. Cambridge Philos. Soc.* **35**, 205 (1939).

¹⁸S. D. Kevan, *Phys. Rev. Lett.* **50**, 526 (1983).

¹⁹D. P. Woodruff, S. L. Hulbert, P. D. Johnson, and N. V. Smith, *Phys. Rev. B* **31**, 4046 (1985).

²⁰G. V. Hanson and S. A. Foldstrom, *Phys. Rev. B* **17**, 473 (1978).

²¹M. Chelvayohan and C. H. B. Mee, *J. Phys. C* **15**, 2305 (1982).

²²F. J. Himpsel and D. E. Eastman, *Phys. Rev. Lett.* **41**, 507 (1978).

²³A. Goldmann, M. Donath, W. Altmann, and V. Dose, *Phys. Rev. B* **32**, 837 (1985).

²⁴E. G. McRae, D. Aberdam, R. Baudoing, and Y. Gauthier, *Surf. Sci.* **74**, 285 (1978).

²⁵P. M. Echenique, F. Flores, and F. Sols, *Phys. Rev. Lett.* **55**, 2348 (1985).

²⁶N. D. Lang and W. Kohn, *Phys. Rev. B* **20**, 873 (1979).

²⁷J. Bausels and P. M. Echenique (unpublished).

²⁸J. R. Manson and R. H. Ritchie, *Phys. Rev. B* **24**, 4867 (1981).

²⁹K. Giesen, F. Hage, F. J. Himpsel, H. J. Riess, and W. Steinmann, *Phys. Rev. B* **33**, 5241 (1986).